https://doi.org/10.5194/egusphere-2026-895
Preprint. Discussion started: 23 April 2026

A Generalized Framework for Multi-Parameter Optimization of Numerical Wind–Wave Model: Application to Typhoon Waves near Taiwan Island

Zongyu Li[2]; Shuiqing Li[1,4]*; Jinrui Chen[3]; Yuan Kong[2]*; Yong Fang[2];Jiageng Han[2]; Pei Zhu[2]; Po Hu[1]

[1]Key Laboratory of Ocean Observation and Forecasting, Key Laboratory of Ocean Circulation and Waves, Institute Oceanology, Chinese Academy of Sciences,Qingdao, 266071, China
[2]College of Mathematics and Systems Science, Shandong University of Science and Technology, Qingdao,266590,China
[3]Fujian Marine Forecasts,Fuzhou,350003.China
[4]University of Chinese Academy of Sciences, Beijing,100049, China

Correspondence to: Shuiqing Li (lishuiqing@qdio.ac.cn); Yuan Kong (kongyuan@sdust.edu.cn)

Abstract. Accurate simulation of typhoon-induced waves is essential for marine hazard forecasting, yet numerical wave models remain limited under extreme wind conditions due to uncertainties in empirically calibrated parameters. In addition, conventional tuning approaches are inefficient for coordinated multi-parameter optimization. This study develops a multi-objective optimization framework for empirical parameter calibration in numerical wave models. Using the WAVEWATCH III model as a testbed, five key parameters influencing offshore and nearshore wave simulations are optimized for typhoon conditions in waters adjacent to Taiwan Island. Latin Hypercube Sampling is used to generate parameter combinations, and batch simulations are evaluated against buoy observations using root mean square error and bias. An adaptive regression model is constructed to map parameter space to error metrics, and the Non-dominated Sorting Genetic Algorithm III (NSGA-III) is applied to identify optimal parameter combinations. Validation with independent typhoon events shows that the optimized configuration effectively improves significant wave height simulations, reducing both RMSE and bias relative to the default scheme. The proposed framework provides an efficient and transferable approach for improving wave model performance under extreme wind conditions.

1 Introduction

Typhoon-induced wind waves, as a major driver of marine disasters, pose severe threats to coastal ecosystems, socio-economic development, and the safety of lives and property. Third-generation spectral wave models, represented by WAVEWATCH III (WW3), have been widely applied in operational typhoon wave forecasting and scientific research. However, the performance of these models depends strongly on the specification of empirical parameters. Many of the parameters that govern key physical processes are still determined on the basis of limited observations or empirical tuning, which introduces substantial uncertainty and constrains the reliability of wave predictions, particularly under extreme wind conditions.

https://doi.org/10.5194/egusphere-2026-895
Preprint. Discussion started: 23 April 2026

Previous studies have conducted sensitivity experiments and regional parameter tuning for source term parameters in the WW3 model, including wind input, wave-wave nonlinear interactions, swell dissipation, and bottom friction.

For instance, empirical parameter tuning is the earliest and most intuitive approach, where researchers directly set or adjust parameter values based on their understanding of physical processes and prior research experience. Apotsos et al. (2008) conducted empirical calibration for natural beaches based on field observations. Rogers et al. (2012) empirically determined wind input and whitecapping dissipation parameters based on Lake George and other observational experiments. Cao et al. (2023), based on physical understanding of drag coefficient saturation under high wind speeds, proposed a new formula using wave age and wave steepness as parameters, reducing mean bias in significant wave height by 91-95%. Raj et al. (2023) determined the optimal CDFAC value of 1.1 based on simulation-observation comparisons under cyclone conditions.

One-At-a-Time (OAT) sensitivity analysis evaluates the influence of individual parameters on simulation results by varying one parameter at a time while keeping others constant. Lee et al. (2009) conducted systematic OAT sensitivity analysis for waters around Taiwan Island, establishing priority rankings for key parameters. Seemanth et al. (2016) found that dissipation parameters have significant influence on wave simulation in the Indian Ocean. Fernández et al. (2021) analyzed ST6 source term parameters for the Irish west coast, finding that CDFAC=0.9 yielded optimal simulation accuracy. Roh et al. (2023) found a positive correlation between CDFAC and simulated significant wave height in East Asian waters.

Multi-factor joint sensitivity analysis simultaneously considers variations in multiple parameters and their interactions, revealing synergistic effects and trade-offs among parameters. Mentaschi et al. (2015) conducted systematic parameter space exploration for the Mediterranean Sea, identifying interdependencies among parameters. Beyramzadeh et al. (2021) constructed a joint error function using both buoy and satellite data for the Persian Gulf, performing joint calibration of multiple parameters.

Optimization algorithm methods employ mathematical optimization techniques to systematically search the parameter space for optimal parameter combinations that minimize objective functions. Gorman & Oliver (2018) applied BOBYQA and ESCH algorithms to simultaneously optimize 17-19 parameters, reducing RMSE by 21% for the ST2 scheme. Kalourazi et al. (2021) used the Newton-Raphson method for iterative optimization of typhoon wave simulation in the Gulf of Mexico, obtaining optimal parameter combinations.

Each method has inherent limitations. Empirically derived parameters are often locally constrained and may lack generalizability. One-at-a-time (OAT) sensitivity analysis neglects parameter interactions, potentially overlooking combined effects on simulation results. Multi-factor joint analyses, while more comprehensive, incur high computational costs and pose challenges for result interpretation. Optimization algorithms are additionally sensitive to subjective choices of objective functions and are prone to convergence toward local optima.

In recent years, data-driven approaches have provided new opportunities for model parameter optimization. Song et al. (2019) demonstrated that deep learning methods can be used to improve parameterization schemes in numerical wave models. Related applications have also emerged in ecosystem and atmospheric modeling (He et al., 2017; Baki et al., 2021).

https://doi.org/10.5194/egusphere-2026-895
Preprint. Discussion started: 23 April 2026

However, in the context of typhoon wave simulations, studies on automated and coordinated multi-parameter optimization remain relatively limited.

To address these challenges, this paper proposes an automated, multi-objective parameter calibration framework for the WW3 wave model based on Latin Hypercube Sampling (LHS), adaptive regression–based surrogate modeling, and the Non-dominated Sorting Genetic Algorithm III (NSGA-III). Using the waters adjacent to Taiwan as a testbed, this study focuses on typhoon wave conditions and applies the proposed framework to jointly calibrate multiple sensitive parameters in the WAVEWATCH III (WW3) model. Section 2 introduces the observational datasets and model configurations. Section 3 presents the parameter optimization methodology, including high-coverage parameter sampling using LHS, construction of a parameter–performance database based on buoy observations, development of an adaptive regression–based surrogate model relation between parameters and error metrics, and application of NSGA-III to identify the optimal parameter combination by simultaneously minimizing RMSE and bias.

2 Methodology and Data

2.1 Study area and typhoon cases

This study focuses on the waters adjacent to Taiwan, with the geographical domain defined as longitude 110° E to130° E and latitude 20° N to 30° N. Observational data from four deep-water buoys and four nearshore shallow-water stations were selected for this research (station locations are shown in Table 1 and Fig. 1). To ensure the robustness and generalizability of the parameter optimization scheme, four typhoon events affecting this region were selected. Four representative typhoons impacting the waters near Taiwan island during 2013–2016 were chosen as case studies, among which Typhoon Dujuan (2015) and Typhoon Megi (2016) were used for parameter training, while Typhoon Fitow (2013) and Typhoon Soudelor (2015) were reserved for independent validation. All four typhoons exhibited northwestward track characteristics, with intensities ranging from severe typhoon to super typhoon, providing good representativeness.

Typhoon Dujuan (1521): Generated over the western Pacific Ocean (15° N, 145.5° E) on September 19, 2015, moving steadily along a northwestward track. It intensified continuously while approaching Taiwan and reached its maximum intensity near the eastern coast of Taiwan island (approximately 23° N, 125° E), with maximum sustained winds of 55 m/s and minimum central pressure of 925 hPa. Subsequently, it crossed Taiwan Island and made landfall on the Fujian coast, weakening rapidly after landfall.

Typhoon Megi (1617): Generated over the western Pacific Ocean (13.3° N, 141.8° E) on September 25, 2016, moving along a west-northwestward track. This typhoon developed rapidly and reached its peak intensity in the waters east of Taiwan Island (approximately 22.7° N, 123.8° E), with maximum sustained winds of 78 m/s and minimum central pressure of 905 hPa, making it the most intense typhoon in this study. After crossing Taiwan Island, it made landfall in Fujian, with intensity decreasing rapidly.

https://doi.org/10.5194/egusphere-2026-895
Preprint. Discussion started: 23 April 2026

Typhoon Fitow (1323): Generated over the ocean east of the Philippines (11° N, 133.7° E) on October 4, 2013, initially moving northward before turning northwestward. Its track was more northerly compared to the other three typhoons. It reached maximum intensity in the southern East China Sea (approximately 23.7° N, 128.5° E), with maximum sustained winds of 68 m/s and minimum central pressure of 910 hPa, then made landfall on the Zhejiang coast, causing severe impacts to the coastal areas of Zhejiang and Fujian.

Typhoon Soudelor (1513): Generated over the far western Pacific Ocean (13.7° N, 160.7° E) on August 1, 2015, with the farthest genesis location from Taiwan Island among the four cases. It intensified rapidly during its long-distance movement along a northwestward track, reaching super typhoon peak intensity over the open ocean (approximately 17.8° N, 140.7° E). Although it weakened somewhat thereafter, it still maintained relatively strong intensity while crossing Taiwan Island, with maximum sustained winds of 60 m/s and minimum central pressure of 935 hPa. It weakened and dissipated after making landfall in Fujian.

The tracks of all four typhoons passed through the Taiwan Strait and its adjacent waters, with peak intensities ranging from severe typhoon to super typhoon. This selection effectively enables the examination of the WW3 model's simulation performance under typhoon wave conditions of varying intensities.

Table 1. Detailed information of eight observation stations

Station	Latitude（° N）	Longitude（° E）	Water Depth（m）
Offshore Buoy1	24.4845	119.2945	70.38
Offshore Buoy2	25.5007	120.3082	49.76
Offshore Buoy3	26.2915	120.7145	64.72
Offshore Buoy4	26.998	121	37.19
Nearshore Buoy1	23.2564	119.6839	20
Nearshore Buoy2	24.0311	121.6325	22
Nearshore Buoy3	22.3161	120.3717	19
Nearshore Buoy4	24.763	121.93	24.5

https://doi.org/10.5194/egusphere-2026-895
Preprint. Discussion started: 23 April 2026

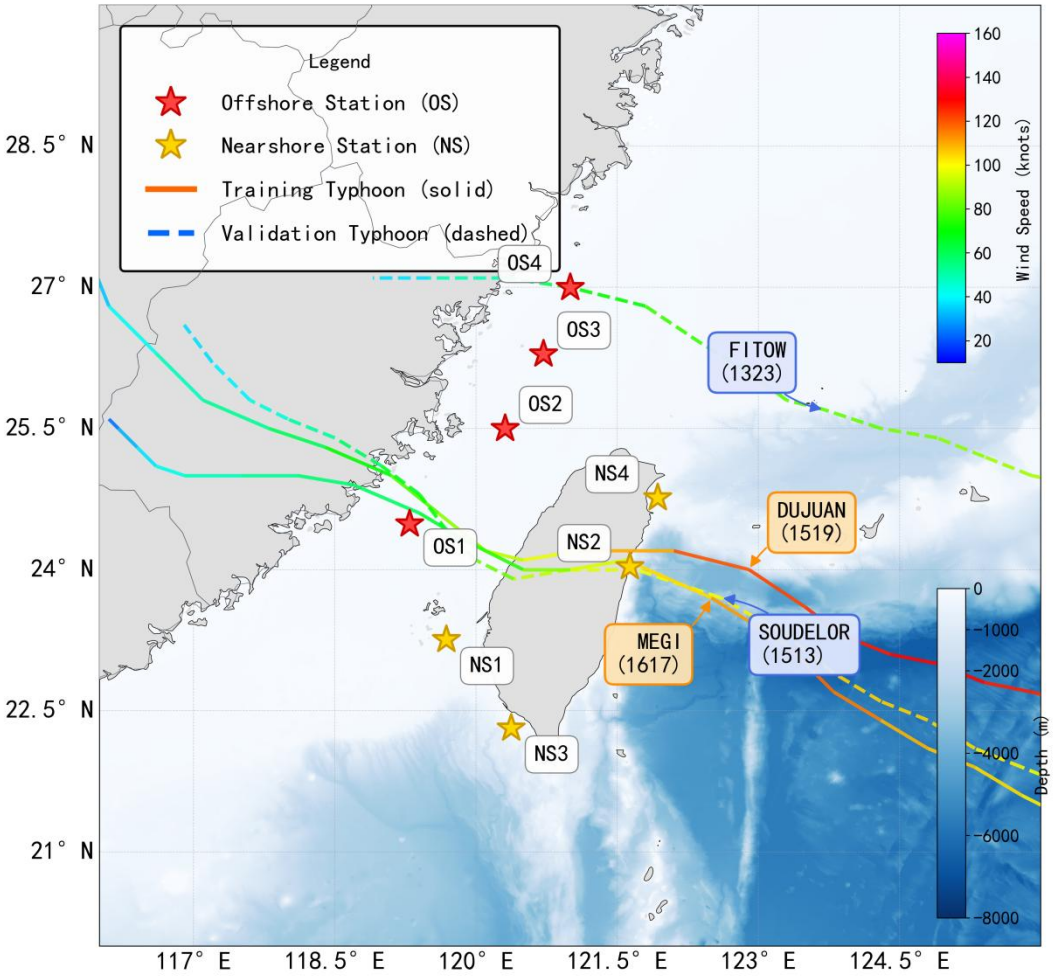

Figure 1. Schematic diagram of the study area, distribution of observation stations, and typhoon tracks. Solid lines indicate typhoon tracks used for training, and dashed lines indicate typhoon tracks used for validation.

2.2 WW3 numerical model configuration

This study employs the third-generation numerical wave model WAVEWATCH III (WW3) version 6.07.1. The WW3 model was developed by the National Oceanic and Atmospheric Administration / National Centers for Environmental Prediction (NOAA/NCEP) of the United States, and is one of the most widely used wave models internationally. It is capable of simulating various physical processes including wave propagation, growth, dissipation, and breaking from deep sea to nearshore areas. The model adopts a spherical coordinate system, with temporal integration using a second-order explicit method. The computational domain covers the northwestern Pacific region, spanning from 116° E to 130° E and 20° N to 30° N, with a spatial resolution of 0.1° × 0.1°.

https://doi.org/10.5194/egusphere-2026-895
Preprint. Discussion started: 23 April 2026

The WW3 model describes the generation, nonlinear transfer, and dissipation processes of wave energy through the source term balance equation. The total source term Stot is composed of multiple physical processes and can be written as:

$$S_{tot} = S_{in} + S_{ds} + S_{nl} + S_{bt} + S_{db} \quad (1)$$

where S_{in} represents the wind energy input term, S_{ds} is the whitecapping dissipation term, S_{nl} denotes the nonlinear wave-wave interactions, and S_{db} is the bottom friction term.

Previous studies have demonstrated that different source term packages have significant impacts on simulation results. Soran et al. (2022) and Hu et al. (2024) compared the differences in significant wave height simulation accuracy among five source term packages (ST1, ST2, ST3, ST4, ST6) in WW3, and conducted sensitivity tests on the adjustable coefficients in each package. The results indicated that different source term packages are suitable for different scenarios: calibrated ST1, ST3, and ST4 perform better in long-term climate simulations, while ST6 yields superior results under extreme wave conditions. Based on the above analysis, this study adopts the ST6 source term package as the baseline configuration for parameter tuning and sensitivity analysis, with the optimal parameter settings presented by Liu et al. (2021) serving as the reference benchmark.The specific tuning parameters selected are shown in Table 2.

Table 2. Key adjustable parameters and their value ranges

Parameter	Physical Meaning	Default Value	Literature Optimal Value	Value Range
SINA0	Negative input factor	0.09	0.05	0.01–1.0
SWLB1	Swell dissipation coefficient	0.0041	0.0041	0.001–0.01
CDFAC	Drag coefficient adjustment factor	1	1.08	0.5–1.5
GAMMA	Friction empirical coefficient	-0.067	-0.067	-0.1–-0.01
BJALFA	Depth-induced breaking coefficient	1	1	0.5–2.0

Negative Wind Input Coefficient (SINA0)

The wind input source term S_{in} describes the process of energy transfer from wind to waves. In the ST6 parameterization scheme, the wind input source term is expressed as (Rogers et al., 2012):

$$S_{in}(k,\theta) = \frac{\rho_a}{\rho_w}\sigma\gamma(k,\theta)N(k,\theta) \quad (2)$$

where ρ_a and ρ_w are the air and seawater densities, respectively, σ is the angular frequency, γ is the wave growth rate, and $N(k,\theta)$ is the wave action spectral density. The growth rate γ is related to the wind speed projection factor W, which is decomposed into the downwind component W_1 and the upwind component W_2:

$$W = W_1 - a_0 W_2 \quad (3)$$

$$W_1 = \max\left\{0, \frac{U}{c}\cos(\theta - \theta_w) - 1\right\}, W_2 = \min\left\{0, \frac{U}{c}\cos(\theta - \theta_w) - 1\right\} \quad (4)$$

https://doi.org/10.5194/egusphere-2026-895
Preprint. Discussion started: 23 April 2026

where U is the wind speed, c is the phase velocity, and θ and θ_w are the wave direction and wind direction, respectively. The coefficient a_0 (i.e., SINA0) controls the intensity of negative wind input, with its default value increasing from 0.04 in v4.18 to 0.09 in v6.07 (WW3DG, 2019).

Swell Dissipation Coefficient (SWLB1)

The swell dissipation source term S_{swl} describes the energy decay process caused by the interaction between swell and ocean turbulence (Babanin, 2011). In the ST6 scheme, swell dissipation is expressed as:

$$S_{swl}(k,\theta) = -\frac{2}{3} b_1 \sigma \sqrt{B_n} N(k,\theta) \tag{5}$$

where σ is the angular frequency, B_n is the spectral saturation, $N(k,\theta)$ is the wave action spectral density, and b_1 is the dissipation intensity coefficient. To reduce spatial bias in wave height, the ST6 scheme introduces steepness dependence (WW3DG, 2019):

$$b_1 = B_1 \cdot 2\sqrt{E} \cdot k_p \tag{6}$$

where E is the total sea surface variance and k_p is the spectral peak wavenumber. The coefficient B_1 (i.e., SWLB1) controls the swell dissipation intensity, with its default value increasing from 2.5×10^{-4} in v4.18 to 4.1×10^{-3} in v6.07 (WW3DG, 2019).

Drag Coefficient Scaling Factor (CDFAC)

The sea surface drag coefficient C_d determines the efficiency of momentum transfer from wind to ocean. In the ST6 scheme, the drag coefficient adopts the parameterized form proposed by Hwang (2011):

$$C_d \times \mathrm{FAC} = 8.058 + 0.967\, U_{10} - 0.016\, U_{10}^2 \tag{7}$$

where U_{10} is the wind speed at 10 m height, and FAC is the adjustable parameter CDFAC. This parameterization accounts for the saturation and decay characteristics of sea surface drag under high wind speed conditions (>30 m/s). This parameter can be used to eliminate systematic biases in different reanalysis wind field products (Ardhuin et al., 2011). The default value of CDFAC is 1.0.

Bottom Friction Coefficient (GAMMA)

The bottom friction source term S_{bot} describes the energy dissipation of waves caused by seafloor friction in shallow water areas. WW3 adopts an empirical linear parameterization scheme derived from the JONSWAP experiment (Hasselmann et al., 1973; WAMDIG, 1988), with the mathematical expression:

$$S_{bot}(k,\theta) = 2\Gamma \frac{n - 0.5}{gd} N(k,\theta) \tag{8}$$

where $n = C_p/C_g$ is the ratio of phase velocity to group velocity, g is gravitational acceleration, d is water depth, and $N(k, \theta)$ is the wave action spectral density. Γ (i.e., GAMMA) is the empirical bottom friction coefficient that controls the bottom friction dissipation intensity. This source function is inversely proportional to water depth, playing a dominant role in

https://doi.org/10.5194/egusphere-2026-895
Preprint. Discussion started: 23 April 2026

shallow water areas. Hasselmann et al. (1973) derived $\Gamma = -0.038$ m²s⁻³ based on swell conditions, while Bouws and Komen (1983) obtained $\Gamma = -0.067$ m²s⁻³ for wind-wave conditions, with the latter being the default value in WW3.

Depth-Induced Breaking Coefficient (BJALFA)

The depth-induced breaking source term S_{db} describes the energy dissipation caused by wave breaking due to depth limitation in shallow water areas. WW3 adopts the Battjes and Janssen (1978) parameterization scheme, assuming that the total dissipation is uniformly distributed across the entire spectrum (Eldeberky and Battjes, 1996). Its mathematical expression is:

$$S_{db}(k,\theta) = -0.25\alpha Q_{\mathrm{b}} f_{\mathrm{m}} \frac{H_{\max}^2}{E} F(k,\theta) \tag{9}$$

where Q_{b} is the breaking proportion, f_{m} is the mean frequency, $H_{\max}$ is the maximum wave height, E is the total spectral energy, and $F(k, \theta)$ is the directional-wavenumber spectral density. The coefficient α (i.e., BJALFA) controls the depth-induced breaking dissipation intensity, and its value directly affects the magnitude of S_{db} in a linear manner. This source term plays a dominant role in nearshore shallow water areas and, together with bottom friction dissipation, determines the decay characteristics of waves in nearshore regions. The default value of BJALFA is 1.0.

The above five parameters cover the main physical processes of the source functions in the WW3 model: CDFAC controls the total wind energy input; SINA0 and SWLB1 regulate wind-wave and swell dissipation in deep water areas, respectively; while GAMMA and BJALFA dominate energy dissipation in nearshore shallow water areas. This parameter combination enables simultaneous optimization of significant wave height simulation accuracy in both offshore and nearshore regions from two dimensions: energy input and dissipation.

3 Proposed Parameter Optimization Scheme

This experiment is mainly divided into three stages, as illustrated in Fig.2.

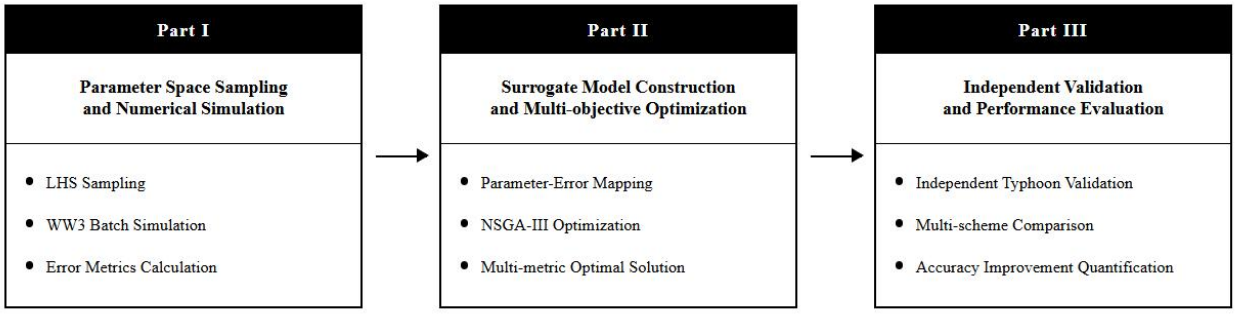

Figure 2. Technical flowchart of the proposed parameter optimization framework

https://doi.org/10.5194/egusphere-2026-895
Preprint. Discussion started: 23 April 2026

3.1 Part I Parameter space sampling and numerical simulation

To explore the high-dimensional parameter space composed of five key parameters (CDFAC, SINA0, SWLB1, GAMMA, BJALFA), this study employs Latin Hypercube Sampling (LHS) to construct the numerical experimental design.

LHS, proposed by McKay et al. (1979), is a stratified random sampling technique designed for high-dimensional problems. The fundamental principle is as follows: for a sampling task involving k parameters and requiring n samples, LHS first divides the range of each parameter into n non-overlapping intervals of equal probability, then randomly selects one sampling point within each interval, and finally randomly combines the sampling points across all parameters to form n parameter sets. This method ensures that each parameter has exactly one sample point in each interval throughout its range, thereby achieving uniform coverage of the parameter space.

Compared with simple random sampling, LHS performs stratified sampling in each parameter dimension, effectively preventing sample clustering in localized regions and significantly improving the coverage efficiency of the parameter space. Compared with regular grid sampling, LHS can ensure global representativeness without requiring dense sampling points in each dimension. If a full factorial design were adopted with 10 levels for each parameter, the five parameters would generate 10^5 = 100,000 combinations, resulting in prohibitive computational costs. In contrast, LHS can effectively characterize response features with considerably fewer samples, substantially reducing the computational burden of numerical simulations.

Following practical experience in surrogate model construction from related fields (Afzal et al., 2017; Davis et al., 2018), a sample size of 100–120 times the parameter dimensions typically ensures sufficient fitting accuracy for surrogate models in a 5-dimensional parameter space. This study selects 600 samples to ensure adequate sampling support in both the boundary regions of the parameter space and local regions with strong nonlinear responses.

For each LHS parameter combination, the WW3 model was run independently for simulation. All experiments adopted identical settings for: model grid and boundary conditions; wind field and initial spectral input; time step and output frequency configurations. To address the issue of underestimated values in ERA5 reanalysis data under high wind speed conditions, a linear correction was introduced. ECMWF systematically underestimates actual wind speeds under high wind conditions (>15 m/s), with the underestimation becoming more severe as wind speed increases. Therefore, the correction magnitude increases linearly with wind speed, and a linear correction is applied using Eq.(10).The correction effect is shown in Fig. 3.

$$U_{\text{corr}} = \begin{cases} U & U \le 15 \\ U + 0.168 \times (U - 15) & U > 15 \end{cases} \tag{10}$$

where U is the original ERA5 wind speed (m/s), U_{corr} is the corrected wind speed (m/s), 15 m/s is the threshold wind speed above which the correction is applied, and 0.168 is the empirical linear correction coefficient derived from observational data calibration by Wu et al. (2025).

https://doi.org/10.5194/egusphere-2026-895
Preprint. Discussion started: 23 April 2026

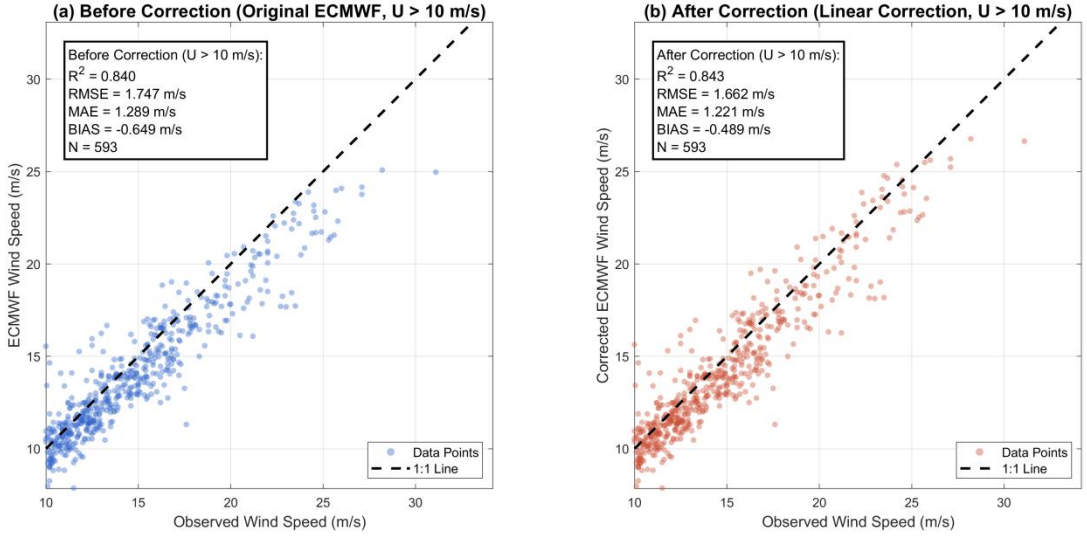

Figure 3. Comparison of ERA5 wind speed before and after linear correction

The model runs were performed using the MPI parallel computing framework, with computational acceleration achieved on a 128-core CPU cluster. A single parameter scheme required approximately 0.3 hours to simulate a 15-day typhoon process, meeting the efficient execution requirements for 600 experimental schemes. The data interaction module was configured as follows:

Input forcing data: Wind fields were derived from ERA5 reanalysis data (spatial resolution of 0.25° × 0.25°, temporal resolution of 1 hour), mapped to the model grid through bilinear interpolation. Bathymetric data were obtained from the ETOPO1 global topography model (resolution of 0.1° × 0.1°), and the bathymetry field for the model grid was generated after depth smoothing processing.

Output and storage configuration: The GRIB package switch was enabled to standardize output data. Core output variables include significant wave height (HS), with a temporal resolution of 1 hour and spatial output range consistent with the computational domain. To meet the validation requirements at observation stations, time series data at 8 target stations were simultaneously output in NetCDF4 format to support rapid calculation of accuracy metrics.

Each simulation outputs the full-field significant wave height, mean period, and directional spectral information. Subsequently, time series data corresponding to observation stations were extracted and compared with measured data. The accuracy metrics calculated include Root Mean Square Error (RMSE) and Bias:

$$\mathrm{RMSE} = \sqrt{\frac{1}{n}\sum_{i=1}^{n}(H_{\mathrm{s},i}^{\mathrm{sim}} - H_{\mathrm{s},i}^{\mathrm{obs}})^2}\ . \tag{11}$$

$$\mathrm{Bias} = \frac{1}{n}\sum_{i=1}^{n}(H_{\mathrm{s},i}^{\mathrm{sim}} - H_{\mathrm{s},i}^{\mathrm{obs}}) \tag{12}$$

https://doi.org/10.5194/egusphere-2026-895
Preprint. Discussion started: 23 April 2026

Through the above 600 experimental results, a parameter-accuracy relationship database can be established, providing data support for subsequent parameter optimization based on Adaptive Regression Model and multi-objective optimization.

3.2 Part II Surrogate model construction and multi-objective optimization

To establish the nonlinear mapping relationship between key parameters of the WW3 model and simulation accuracy metrics (RMSE, Bias), this study introduces an adaptive regression model library as the surrogate model. A surrogate model is an approximate modeling method based on statistical regression or machine learning, which learns the input-output relationship from limited sample data to avoid the high computational cost of repeated numerical model simulations. The model library constructed in this study encompasses two major categories of methods: traditional statistical regression models, including linear regression, ridge regression, Lasso regression, elastic net, and polynomial regression; and machine learning regression models, including support vector regression, decision tree, random forest, gradient boosting trees (XGBoost, LightGBM), and feedforward neural networks.

Based on the initial model library, this study adopts an adaptive modeling strategy to achieve optimal predictive performance. First, for the key hyperparameters of each model (such as kernel parameters for support vector machines, tree depth for random forests, and learning rate for gradient boosting trees), tuning was performed using a combination of grid search and Bayesian optimization, with L1/L2 regularization introduced to control model complexity and prevent overfitting. Second, input parameters were progressively screened through incremental feature selection methods, comparing validation errors under different feature combinations to identify the parameter subset with the greatest contribution to prediction accuracy. Finally, the predictive performance of each model was evaluated through cross-validation, and the best-performing model was automatically selected as the primary surrogate model. If multiple models exhibited similar performance, a performance-based weighted averaging strategy was employed to ensemble multi-model predictions, thereby reducing the uncertainty of individual models and improving the robustness and generalization capability of the surrogate model.

Based on the parameter-accuracy relationship database obtained from 600 experimental results, the adaptive regression library was utilized to construct parameter-accuracy surrogate models for each station. The specific fitting accuracy and comparisons between actual values and predicted values for selected models are shown below.

Table 3. Accuracy of adaptive model library

Station	Metric	Optimal Model	R^2	RMSE	MAE
Offshore 1	RMSE_m	Poly3_Ridge	0.993916	0.020551	0.017657
Offshore 1	Bias_m	Poly2_Ridge	0.977727	0.062744	0.052462
Offshore 2	RMSE_m	Poly3_Ridge	0.754237	0.102354	0.089075
Offshore 2	Bias_m	Poly2_Ridge	0.901721	0.144826	0.142984
Offshore 3	RMSE_m	Poly3_Ridge	0.963886	0.039807	0.031799
Offshore 3	Bias_m	Poly2_Ridge	0.988360	0.047916	0.044757
Offshore 4	RMSE_m	Poly3_Ridge	0.859744	0.077741	0.069508

https://doi.org/10.5194/egusphere-2026-895
Preprint. Discussion started: 23 April 2026

Offshore 4	Bias_m	Poly2_Ridge	0.960803	0.071239	0.070113
Nearshore 1	RMSE_m	SVR_RBF	0.838838	0.090569	0.086111
Nearshore 1	Bias_m	Poly2_Ridge	0.984288	0.050226	0.042286
Nearshore 3	RMSE_m	Poly2_Ridge	0.980236	0.136257	0.112386
Nearshore 3	Bias_m	Ridge	0.947279	0.083326	0.109535

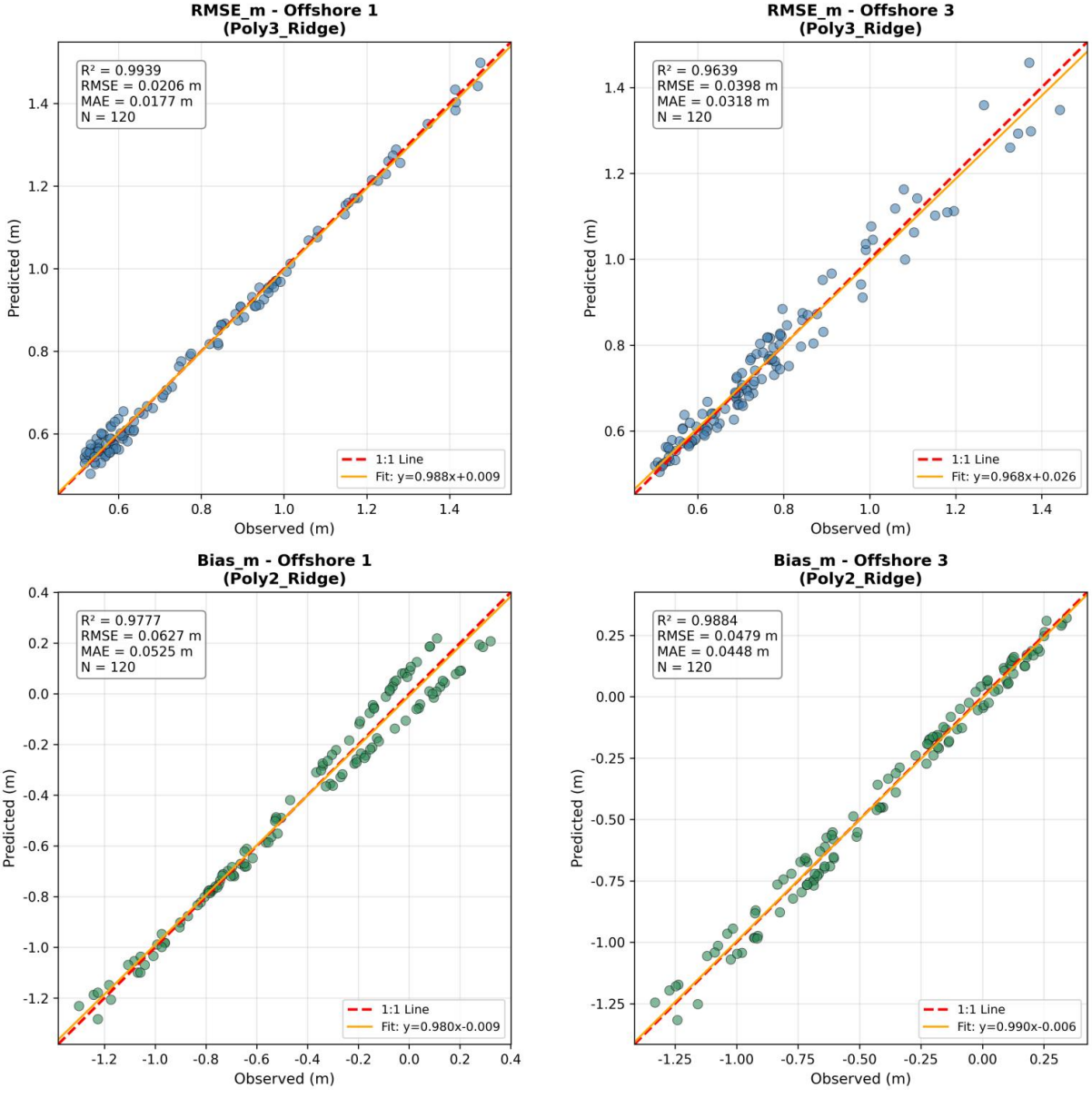

https://doi.org/10.5194/egusphere-2026-895
Preprint. Discussion started: 23 April 2026

Figure 4. Accuracy results of adaptive regression library for selected stations

As shown in Fig.4, the surrogate models constructed through the adaptive regression library can effectively represent the nonlinear mapping relationship between parameters and simulation accuracy metrics (RMSE, Bias). To further validate the accuracy of the nonlinear mapping relationship models, two randomly selected parameter combinations were evaluated using both the nonlinear mapping model and the WW3 numerical model. The specific output RMSE and Bias values are shown in Table 4.

Table 4. Accuracy comparison for two randomly selected parameter combinations (where SMPA denotes Surrogate Model Prediction Accuracy, and NMSA denotes Numerical Model Simulation Accuracy)

Station	Group 1 RMSE		Group 1 Bias		Group 2 RMSE		Group 2 Bias	
	SMPA	NMSA	SMPA	NMSA	SMPA	NMSA	SMPA	NMSA
Nearshore 1	0.8514	0.8419	0.3036	0.3344	0.9266	0.9693	0.378	0.0807
Nearshore 3	0.7551	0.7617	-0.0563	-0.046	0.8286	0.8395	-0.0112	-0.0407
Offshore 1	0.5718	0.5217	-0.2466	-0.23	0.5723	0.5476	-0.1739	-0.1413
Offshore 2	0.5814	0.5647	-0.1554	-0.1866	0.6307	0.6948	-0.0779	-0.0722
Offshore 3	0.5262	0.5652	-0.1687	-0.1296	0.5678	0.5319	-0.114	-0.1662
Offshore 4	0.3601	0.3919	-0.127	-0.13	0.367	0.4666	-0.0469	-0.0493

The comparison table demonstrates that the surrogate model predictions for RMSE and Bias are in excellent agreement with actual values, with very small overall prediction errors. This validates the reliability of the surrogate model and demonstrates that the constructed surrogate model can accurately characterize the nonlinear coupling relationships among parameters, effectively replacing time-consuming numerical model simulations.

After obtaining the high-accuracy surrogate model, it serves as an approximate substitute for the objective function of the numerical model to construct a multi-objective optimization problem, thereby achieving the optimal combination solution for key parameters of the WW3 model. The surrogate model enables rapid prediction of simulation errors corresponding to different parameter combinations without repeatedly running the numerical model, thus significantly reducing optimization computational cost.

The optimization objective is to obtaining a set of parameter schemes with minimal simulation error,. Specifically, the two optimization objectives are:

$f_1(\boldsymbol{x})$: Root mean square error of simulated significant wave height (RMSE) (13)

$f_2(\boldsymbol{x})$: Absolute bias of simulated significant wave height (|Bias|) (14)

Let $\boldsymbol{x}=[x_1, x_2, x_3, x_4, x_5]$represent the five parameters to be optimized (SINA0, SWLB1, CDFAC, GAMMA, BJALFA). The multi-objective optimization problem can be formulated as:

$$\min_{\boldsymbol{x}} \boldsymbol{F}(\boldsymbol{x}) = [f_1(\boldsymbol{x}), f_2(\boldsymbol{x})] = [\mathrm{RMSE}(\boldsymbol{x}), |\mathrm{Bias}(\boldsymbol{x})|]$$

https://doi.org/10.5194/egusphere-2026-895
Preprint. Discussion started: 23 April 2026

$$\text{s.t.}\begin{cases} x_3 \in [0.5,1.5], \end{cases} \tag{15}$$

This problem belongs to the category of Nonlinear Multi-objective Optimization Problems (MOP). In multi-objective optimization, there typically does not exist a single solution that simultaneously optimizes all objectives. An example is given for CDFAC. Uniform discrete sampling is performed within the parameter constraint range $[\theta_k^{\min}, \theta_k^{\max}]$:

$$\theta_k^{(i)} = \theta_k^{\min} + \frac{i-1}{n-1} \cdot (\theta_k^{\max} - \theta_k^{\min}),\ i = 1,2,...,n \tag{16}$$

where n is the number of sampling points. In this study, $n = 100$ is adopted. For the CDFAC parameter, the sampling range is set as $\theta_k^{\min} = 0.5$ and $\theta_k^{\max} = 1.5$. For each sampling point, only the target parameter is varied while all other parameters are fixed at their baseline values from the optimal solution, constructing the parameter vector:

$$\boldsymbol{\theta}^{(i)} = \left(\theta_1^{\text{base}}, ..., \theta_{k-1}^{\text{base}}, \theta_k^{(i)}, \theta_{k+1}^{\text{base}}, ..., \theta_5^{\text{base}}\right)^{\mathrm{T}} \tag{17}$$

The prediction errors at each station are calculated through the surrogate model, and the mean values are obtained:

$$\overline{\text{RMSE}}^{(i)} = \frac{1}{N_s}\sum_{s=1}^{N_s} \text{RMSE}_s(\boldsymbol{\theta}^{(i)}),\ \overline{|\text{Bias}|}^{(i)} = \frac{1}{N_s}\sum_{s=1}^{N_s} |\text{Bias}_s(\boldsymbol{\theta}^{(i)})| \tag{18}$$

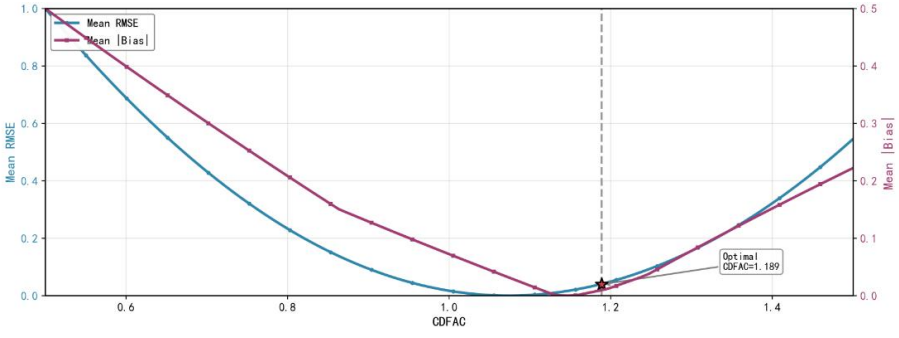

Figure 5. Error metric curve of CDFAC parameter

The results indicate that both RMSE and |Bias| exhibit a "U-shaped" response characteristic with an initial decrease followed by an increase, with the optimal range located near CDFAC ≈ 1.2. When CDFAC < 1.0, both metrics decrease significantly as the parameter increases, indicating that insufficient wind energy input leads to systematic underestimation of simulated wave heights. When CDFAC > 1.2, the metrics begin to rise again, indicating that excessive wind energy input causes wave height overestimation. This study employs the Non-dominated Sorting Genetic Algorithm III (NSGA-III) for solving. The optimal solution yields CDFAC = 1.189. As shown in Fig. 5, this value does not correspond to the minimum RMSE or Bias for CDFAC alone. This is attributed to the interdependencies among all five parameters. The optimal result is not determined by any single parameter individually, but rather reflects the nonlinear coupling relationships among multiple parameters.

https://doi.org/10.5194/egusphere-2026-895
Preprint. Discussion started: 23 April 2026

Based on the constructed optimization model, solutions achieving a good balance between RMSE and Bias were obtained. The specific parameters are shown in Table 5.

Table 5. Parameter values for each scheme

Parameter	Literature Values	Default Values	Optimal Parameters	Corrected Wave Height Optimal Parameters
SINA0	0.05	0.09	0.0115	0.5189
SWLB1	0.0041	0.0041	0.0089	0.0056
CDFAC	1.08	1	1.189	1.126
GAMMA	-0.067	-0.067	-0.049	-0.0373
BJALFA	1	1	1.499	0.692

As illustrated in the next section, CDFAC and GAMMA emerge as the most sensitive parameters affecting the simulations. The optimal value of the drag coefficient scaling factor CDFAC is 1.189, representing an increase of approximately 19% compared to the default value. This parameter directly controls the magnitude of the sea surface drag coefficient Cd, thereby regulating the efficiency of energy transfer from wind to waves. The enhanced CDFAC implies stronger wind energy input than in the default configuration, which may attributed to limited wind fetch in this region, leading to enhanced wind drag (e.g. Li 2023). The optimal value of the bottom friction coefficient GAMMA is −0.049, which falls between the values reported in the literature: −0.038 for swell conditions and −0.067 for wind-sea conditions.

3.3 Part III Independent validation and performance evaluation

To more clearly demonstrate the improvement of the optimized parameter set, we conducted numerical simulations using the optimized parameters and compared the results with those obtained using the default and literature-recommended parameter schemes. The corresponding results are summarized in Table 6.

Table 6. Accuracy comparison among three parameter schemes

Station	Parameter Scheme	RMSE	MAE	Bias	Station	Parameter Scheme	RMSE	MAE	Bias
Offshore 1	Default	0.603	0.474	-0.336	Offshore 4	Default	0.393	0.305	-0.2
	Literature	0.541	0.425	-0.205		Literature	0.384	0.287	-0.089
	Optimal	0.528	0.398	-0.069		Optimal	0.289	0.218	-0.095
Offshore 2	Default	0.59	0.53	-0.398	Nearshore 1	Default	0.508	0.388	-0.123
	Literature	0.561	0.478	-0.261		Literature	0.505	0.385	0.005
	Optimal	0.501	0.378	-0.106		Optimal	0.532	0.399	0.136
Offshore 3	Default	0.548	0.478	-0.327	Nearshore 3	Default	0.499	0.372	-0.335
	Literature	0.544	0.435	-0.185		Literature	0.44	0.32	-0.247
	Optimal	0.52	0.37	-0.009		Optimal	0.389	0.282	-0.138

https://doi.org/10.5194/egusphere-2026-895
Preprint. Discussion started: 23 April 2026

The table demonstrates that the optimal parameters outperform the other two parameter schemes across all stations in terms of RMSE, MAE, and Bias. The mean RMSE across all stations decreased from 0.53 m to 0.46 m, and the mean Bias improved from -0.29 m to -0.047 m. To more intuitively illustrate the accuracy improvement, we plotted the time series for several representative stations, as shown in Fig. 6.

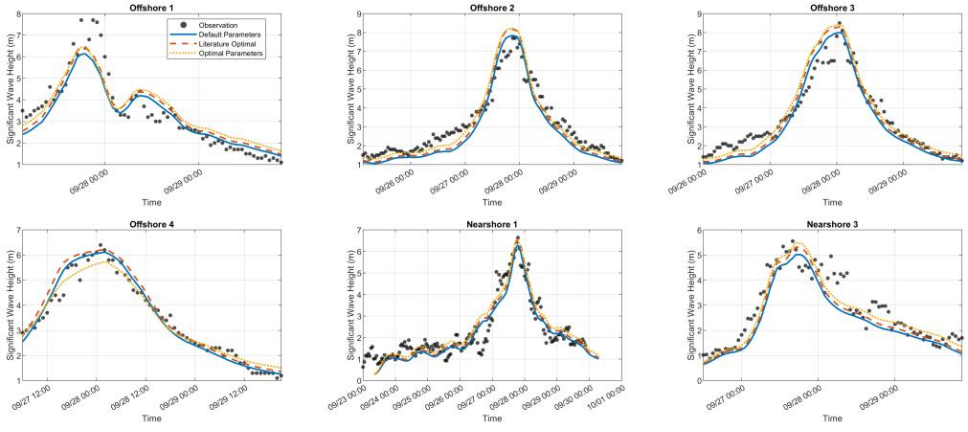

Figure 6. Time series comparison of simulation results among three parameter schemes

To verify the accuracy and generalizability of the optimal model parameters, the optimal parameters were compared with default parameters and literature optimal parameters using the validation set typhoons, including Typhoon Soudelor and Typhoon Fitow. The specific results are shown in Table 7.

Table 7. Comparison of simulation performance among different parameter schemes for validation typhoons

Station	Parameter Scheme	Typhoon Soudelor (Validation)			Typhoon Fitow (Validation)		
		RMSE (m)	MAE (m)	Bias (m)	RMSE (m)	MAE (m)	Bias (m)
Offshore 2	Default	0.283	0.214	-0.157	0.581	0.442	-0.414
	Literature Optimal	0.271	0.2	-0.069	0.448	0.315	-0.222
	Optimized	0.324	0.201	0.045	0.437	0.342	0.027
Offshore 3	Default	0.382	0.307	-0.283	0.903	0.735	-0.728
	Literature Optimal	0.313	0.243	-0.178	0.719	0.551	-0.524
	Optimized	0.297	0.201	-0.039	0.569	0.413	-0.258
Offshore 4	Default	0.521	0.4	-0.381	0.497	0.378	-0.156
	Literature Optimal	0.45	0.334	-0.298	0.473	0.339	-0.007
	Optimized	0.428	0.28	-0.244	0.46	0.327	0.096
Nearshore 1	Default	0.346	0.289	-0.285	0.603	0.48	-0.422
	Literature Optimal	0.303	0.249	-0.218	0.48	0.381	-0.258
	Optimized	0.289	0.241	-0.14	0.392	0.314	-0.012

https://doi.org/10.5194/egusphere-2026-895
Preprint. Discussion started: 23 April 2026

The Nearshore 2 station exhibits the most substantial improvement, with RMSE decreasing from 0.60 m (default) and 0.48 m (literature optimal) to 0.39 m, corresponding to reductions of 35% and 18%, respectively. At the Offshore 3 station, RMSE decreases from 0.38 m (default) and 0.31 m (literature optimal) to 0.30 m, yielding the best overall performance among all parameter schemes.

The most pronounced MAE improvement is observed at the Offshore 3 station, where values decrease from 0.31 m (default) and 0.24 m (literature optimal) to 0.20 m, representing reductions of 35% and 17%, respectively. At the Nearshore 2 station, MAE decreases from 0.48 m (default) and 0.38 m (literature optimal) to 0.31 m, consistently maintaining its comparative advantage.

The absolute Bias values at all stations converge toward zero after optimization. At the Nearshore 2 station, Bias improves from −0.42 m (default) and −0.26 m (literature optimal) to approximately zero (−0.012 m), effectively eliminating systematic bias. At the Offshore 2 station, Bias shifts from default underestimation (−0.16 m) to slight overestimation (0.045 m), with Bias constrained within ±0.05 m, indicating markedly improved stability.To further validate the results, we present comparisons between simulated and observed values before and after parameter adjustment, as shown in Figs. 7 and 8.

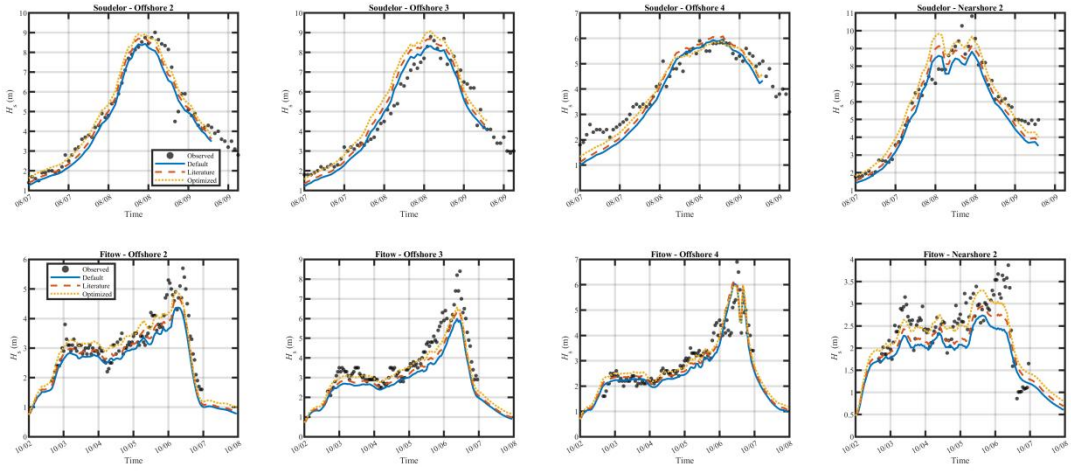

Figure 7. Time series of validation typhoons

https://doi.org/10.5194/egusphere-2026-895
Preprint. Discussion started: 23 April 2026

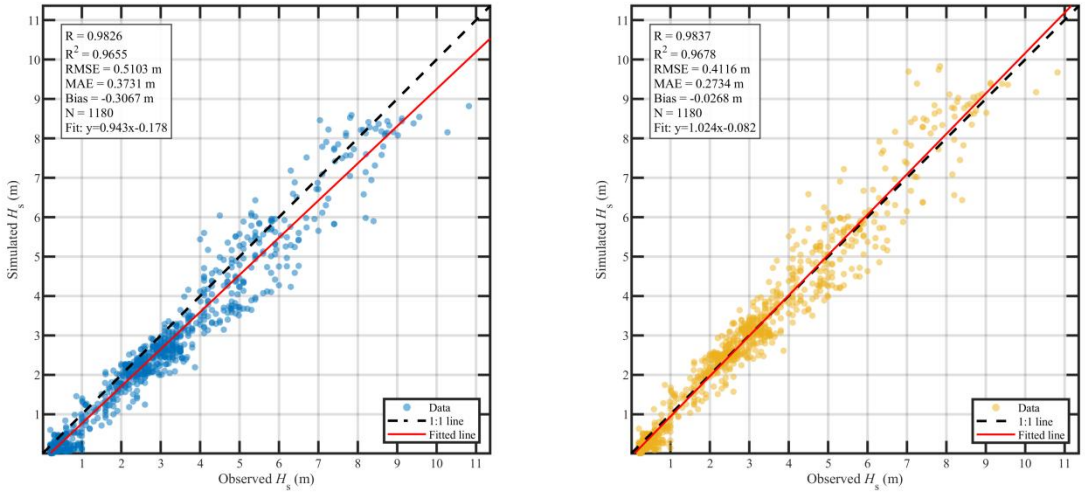

Figure 8. Scatter plots before and after parameter optimization

The simulation results with default parameters show a correlation coefficient (R) of 0.98, a Root Mean Square Error (RMSE) of 0.51 m, a Mean Absolute Error (MAE) of 0.37 m, and a Bias of −0.31 m, indicating an obvious systematic underestimation. With the optimized parameters, the RMSE is reduced from 0.51 m to 0.41 m, corresponding to a reduction of 19% relative to the default parameters. The MAE decreases to 0.27 m, with a reduction of 27%, indicating a substantial reduction in overall dispersion. The Bias improves to −0.027 m, with its absolute value reduced by 91% compared to the default case. The scatter plots clearly demonstrate that parameter optimization significantly alleviates the model's underestimation in high wave height regions.

4 Discussion

4.1 Sensitivity analysis

The aforementioned procedure determined the parameter combination with optimal comprehensive accuracy, but the degree of influence of each parameter on simulation results varies. Clarifying parameter sensitivity helps understand the response characteristics of the model. This study applies small-magnitude perturbations to each parameter near the optimal solution and quantifies the local sensitivity of each parameter by observing the relative changes in the objective function.

A sensitivity coefficient (elasticity coefficient) is introduced, defined as:

$$S_k = \frac{\partial y / y}{\partial \theta_k / \theta_k} \approx \frac{\Delta y / y^{\text{base}}}{\Delta \theta_k / \theta_k^{\text{base}}} \tag{19}$$

where θ_k is the parameter at position k, y is the objective function (RMSE or Bias), and the superscript "base" denotes the baseline value at the optimal solution. This coefficient represents the relative response amplitude of the objective function

https://doi.org/10.5194/egusphere-2026-895
Preprint. Discussion started: 23 April 2026

when the parameter changes by 1%. A larger absolute value indicates greater model sensitivity to that parameter. Perturbations of different magnitudes (1%, 5%, 10%) are applied to each parameter. For all perturbations of each parameter (3 magnitudes × 2 directions = 6 times), the average sensitivity is calculated. The average sensitivities for RMSE and Bias are computed separately, and then the comprehensive sensitivity is obtained:

$$\bar{S}_i^{\text{comprehensive}} = \frac{\bar{S}_i^{\text{RMSE}} + \bar{S}_i^{\text{Bias}}}{2} \tag{20}$$

The overall parameter sensitivity under different perturbations is summarized in Table 8. The sensitivity analysis identifies CDFAC as the most influential parameter, highlighting the dominant role of wind energy input. Bottom friction and depth-induced breaking follow in importance, with bottom friction having a slightly greater impact, which may be attributed to the fact that the selected buoys are not located very close to the shore. The effects of SWLB1 and SINA0 are relatively minor, likely because the selected data primarily represent the typhoon core or wind-limited regions, where the influence of swell is weak. These findings are in good agreement with the conclusions of Roh et al. (2023).

Table 8. Parameter sensitivity ranking

Parameter	Sensitivity
CDFAC	2.8149
GAMMA	0.4145
BJALFA	0.1441
SWLB1	0.0214
SINA0	0.0002

4.2 Wind speed influence

In addition to uncertainties inherent in the numerical model, the accuracy of the wind field represents another major source of uncertainty in typhoon wind wave simulations. The performance of wave models is highly dependent on the quality of the input wind fields. It is well known that ERA5 tends to underestimate extreme wind speeds, despite well representing the typhoon horizontal wind structure. Although we have applied a statistical corrections to mitigate this bias, the errors cannot be completely eliminated, let alone the scatter. Consequently, parameter tuning is inevitably influenced by the choice of wind field. To account for this effect, we apply a normalization method based on the squared wind speed ratio to adjust the simulated wave heights.

According to classical wind-wave growth theory , under fully developed deep-water wind-wave conditions, significant wave height Hs is approximately proportional to the square of wind speed U, as shown in Fig. 9:

$$H_s \propto U^2 \tag{21}$$

https://doi.org/10.5194/egusphere-2026-895
Preprint. Discussion started: 23 April 2026

Let the simulated wave height $H_{s,mod}$ be driven by ERA5 wind speed U_{ERA5}, and the observed significant wave height $H_{s,true}$ correspond to observed wind speed U_{obs}. Then:

$$H_{s,mod} \propto U_{ERA5}^2 \tag{22}$$

$$H_{s,true} \propto U_{obs}^2 \tag{23}$$

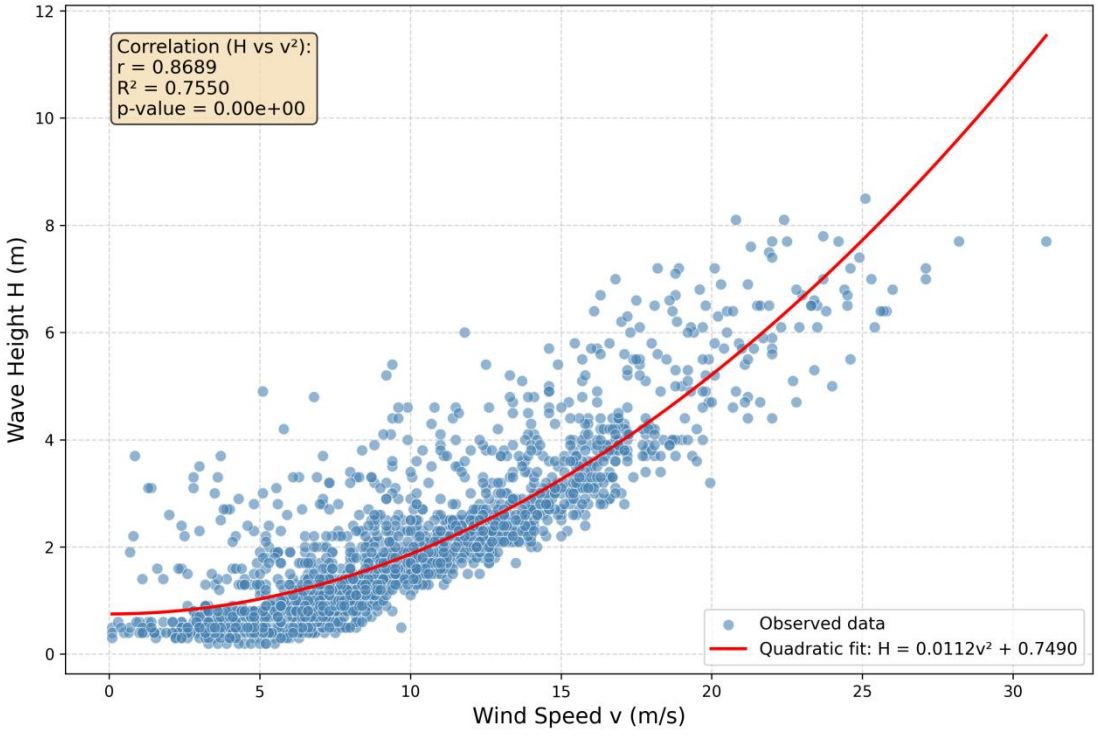

Figure 9. The relationship between observed significant wave height and observed wind speed from buoy data

Dividing the two equations yields:

$$\frac{H_{s,true}}{H_{s,mod}} = \frac{U_{obs}^2}{U_{ERA5}^2} \tag{24}$$

Rearranging gives the correction formula:

$$H_{s,corrected} = H_{s,mod} \times \frac{U_{obs}^2}{U_{ERA5}^2} \tag{25}$$

We used the corrected simulated wave heights, Hs,corrected, in place of Hs,mod within the parameter optimization framework to derive the optimized parameter values, as summarized in Table 5. CDFAC decreased slightly from 1.189 to 1.126 (≈5% reduction), suggesting that the choice of wind field has a limited impact on the wind input factor. In contrast, other parameters underwent varying degrees of adjustment, with some showing substantial changes (e.g., SINA0). This is

https://doi.org/10.5194/egusphere-2026-895
Preprint. Discussion started: 23 April 2026

attributed to that these parameters are considerably less sensitive than CDFAC, so their optimal values are not strongly constrained, and changes in these parameters have little effect on the overall simulation performance.

5 Conclusions

This study presents a multi-objective parameter calibration framework for the numerical wind-wave model, designed to systematically address parameter uncertainty in typhoon wave simulations. By integrating Latin Hypercube Sampling (LHS), adaptive regression–based surrogate modeling, and NSGA-III multi-objective optimization algorithm, the proposed framework enables efficient exploration of high-dimensional parameter spaces and coordinated optimization of multiple accuracy metrics.

Application of the framework to typhoon wave simulations in the waters adjacent to Taiwan island demonstrates that the optimized parameter set effectively improves the simulation of significant wave height compared to both default and literature-recommended parameter configurations. Independent validation using additional typhoon cases confirms the robustness of the optimized parameters, with notable reductions in RMSE and near-elimination of systematic bias. Sensitivity analysis further indicates that wind energy input (CDFAC) is the dominant controls on model performance under extreme wind–wave conditions in coastal regions. These results demonstrate that the framework can be used to diagnose the dominant physical mechanisms governing wave evolution. Future studies could consider a region-specific approach (e.g., areas away from the storm core) to enhance the sensitivity of other parameters and apply this framework to determine their optimal values.

Beyond the specific case study, the proposed optimization framework is model-agnostic and transferable. At the model level, it can be readily extended to other source-term packages within WW3 (e.g., ST4) and to other third-generation wave models such as SWAN and WAM. At the regional level, provided that in situ or satellite-based wave observations are available, the same workflow can be applied to derive regionally optimized parameter sets, thereby improving model performance in diverse coastal and open-ocean environments.

Several limitations of this study should be acknowledged. First, parameter calibration primarily mitigates systematic model biases and cannot fundamentally resolve deficiencies inherent to the underlying physical parameterizations. Second, the optimized parameter set is specifically tuned for typhoon conditions, and its applicability to moderate or climatological wind–wave regimes remains to be systematically evaluated. Third, the calibrated results may retain a degree of regional dependence related to local bathymetry, wind forcing characteristics, and observational constraints.

Future work will focus on extending the proposed framework to the coordinated calibration of multiple feature parameters, incorporating additional wave characteristics beyond significant wave height, such as the dominant wave period and the wave spectrum.

https://doi.org/10.5194/egusphere-2026-895
Preprint. Discussion started: 23 April 2026

Code and data availability.

The multi-objective parameter optimization framework developed in this study, including Latin Hypercube Sampling scripts, adaptive regression surrogate models, and NSGA-III optimization algorithms, is publicly available. The repository also contains typhoon wave buoy observations, WAVEWATCH III configuration files, and trained surrogate model outputs. All code and data are archived on Figshare at https://doi.org/10.6084/m9.figshare.31236334 (Li et al., 2025). The WAVEWATCH III model (version 6.07) is available from the NOAA/NCEP repository (https://github.com/NOAA-EMC/WW3; WW3DG, 2019). ERA5 reanalysis data used for wind forcing were obtained from the Copernicus Climate Data Store (https://cds.climate.copernicus.eu/).

Author contributions

SL conceptualized this study. ZL conducted the experiments and data analysis, and developed the model code. SL and ZL prepared the manuscript. JC provided the buoy data. YK, YF, JH, PZ, and PH provided valuable comments on the project.

Competing interests

The contact author has declared that none of the authors has any competing interests.

Disclaimer

Publisher's note: Copernicus Publications remains neutral with regard to jurisdictional claims made in the text, published maps, institutional affiliations, or any other geographical representation in this paper. While Copernicus Publications makes every effort to include appropriate place names, the final responsibilitylies with the authors.

Acknowledgements

This study was supported by the Na tional Key Research and Development Program of China (2023YFC3008200). Thanks for the computing support from the Oceanographic Data Center, Chinese Academy of Sciences (http://msdc.qdio.ac.cn).

References

Afzal, A., Kim, K. Y., and Seo, J. W.: Effects of Latin hypercube sampling on surrogate modeling and optimization, Int. J. Fluid Mach. Syst., 10, 240–253, https://doi.org/10.5293/IJFMS.2017.10.3.240, 2017.

Apotsos, A., Raubenheimer, B., Elgar, S., Guza, R. T., and Smith, J. A.: Testing and calibrating parametric wave transformation models on natural beaches, Coast. Eng., 55, 224–235, https://doi.org/10.1016/j.coastaleng.2007.10.002, 2008.

https://doi.org/10.5194/egusphere-2026-895
Preprint. Discussion started: 23 April 2026

Ardhuin, F., Hanafin, J., Quilfen, Y., Chapron, B., Queffeulou, P., Obrebski, M., Sienkiewicz, J., and Vandermark, D.: Calibration of the IOWAGA global wave hindcast (1991–2011) using ECMWF and CFSR winds, in: Proceedings of the 12th International Workshop on Wave Forecasting and Hindcasting, 1–13, 2011.

Babanin, A., Hsu, T.-W., Roland, A., Ou, S.-H., Doong, D.-J., and Kao, C.: Spectral wave modelling of Typhoon Krosa, Nat. Hazards Earth Syst. Sci., 11, 501–511, https://doi.org/10.5194/nhess-11-501-2011, 2011.

Baki, H., Chinta, S., Balaji, C., and Srinivasan, B.: WRF model parameter calibration to improve the prediction of tropical cyclones over the Bay of Bengal using Machine Learning-based Multiobjective Optimization, arXiv [preprint], https://doi.org/10.48550/arXiv.2110.05817, 12 October 2021.

Battjes, J. A. and Janssen, J. P. F. M.: Energy loss and set-up due to breaking of random waves, in: Proceedings of the 16th International Conference on Coastal Engineering, Hamburg, Germany, 27 August – 3 September 1978, ASCE, 569 – 587, https://doi.org/10.9753/icce.v16.32, 1978.

Beyramzadeh, M. and Siadatmousavi, S. M.: Performance evaluation of input-dissipation parameterizations in WAVEWATCH III for Persian Gulf, Ocean Eng., 219, 108374, https://doi.org/10.1016/j.oceaneng.2020.106959, 2021.

Bouws, E. and Komen, G. J.: On the balance between growth and dissipation in an extreme depth-limited wind-sea in the southern North Sea, J. Phys. Oceanogr., 13, 1653–1658, https://doi.org/10.1175/1520-0485(1983)013<1653:OTBBGA>2.0.CO;2, 1983.

Cao, S. C., Zhao, D. L., Guan, C. L., and Sun, J.: Application and improvement of WAVEWATCH III third-generation wave numerical model in the East China Sea, Period. Ocean Univ. China (Nat. Sci. Ed.), 53(8), 1 – 10, https://doi.org/10.16441/j.cnki.hdxb.20220118, 2023 (in Chinese).

Chen, T. C. and Collet, F.: Evaluation of ERA5 precipitation and 10-m wind speed associated with extratropical cyclones using station data over North America, Int. J. Climatol., 44, 825–844, https://doi.org/10.1016/j.jhydrol.2020.125660, 2024.

Christensen, T., Pena, A., and Hahmann, A. N.: Underestimation of strong wind speeds offshore in ERA5: evidence, discussion and correction, Wind Energ. Sci., 9, 1727–1745, https://doi.org/10.5194/wes-9-1727-2024, 2024.

Davis, S. E., Cremaschi, S., and Eden, M. R.: Efficient surrogate model development: impact of sample size and underlying model dimensions, Comput. Aided Chem. Eng., 44, 979–984, https://doi.org/10.1016/B978-0-444-64241-7.50158-0, 2018.

Eldeberky, Y.: Nonlinear transformations of wave spectra in the nearshore zone, Ph.D. thesis, Delft University of Technology, Delft, The Netherlands, 203 pp., 1996.

Fernández, L., Calvino, C., and Dias, F.: Sensitivity analysis of wind input parametrizations in the WAVEWATCH III spectral wave model using the ST6 source term package for Ireland, Appl. Ocean Res., 115, 102826, https://doi.org/10.1016/j.apor.2021.102826, 2021.

Gorman, R. M. and Oliver, H. J.: Automated model optimisation using the Cylc workflow engine (Cyclops v1.0), Geosci. Model Dev., 11, 2153–2173, https://doi.org/10.5194/gmd-11-2153-2018, 2018.

Hasselmann, K., Barnett, T. P., Bouws, E., Carlson, H., Cartwright, D. E., Enke, K., Ewing, J. A., Gienapp, H., Hasselmann, D. E., Kruseman, P., Meerburg, A., Müller, P., Olbers, D. J., Richter, K., Sell, W., and Walden, H.: Measurements of wind-

https://doi.org/10.5194/egusphere-2026-895
Preprint. Discussion started: 23 April 2026

wave growth and swell decay during the Joint North Sea Wave Project (JONSWAP), Ergänzungsheft zur Deutschen Hydrographischen Zeitschrift, Reihe A(8), 12, 95 pp., 1973.

Hourdin, F., Mauritsen, T., Gettelman, A., Golaz, J. C., Balaji, V., Duan, Q., Folber, D., Ji, D., Klocke, D., Qian, Y., Raber, F., Rio, C., Tomassini, L., Watanabe, M., and Williamson, D.: The art and science of climate model tuning, Bull. Am. Meteorol. Soc., 98, 589–602, https://doi.org/10.1175/BAMS-D-15-00135.1, 2017.

Hu, Y., Shao, W., Shi, J., Sun, J., Ji, Q., and Cai, L.: Improvement of drag coefficient parameterization of WAVEWATCH-III using remotely sensed products during tropical cyclones, Ocean Dynam., 74, 843–858, https://doi.org/10.1007/s10236-024-01638-3, 2024.

Hwang, P. A.: A note on the ocean surface roughness spectrum, J. Atmos. Ocean. Technol., 28, 436 – 443, https://doi.org/10.1175/2010JTECHO812.1, 2011.

Jiang, X., Mao, M., Liu, Y., and Wang, D.: Evaluation and improvement of the ERA5 wind field in typhoon storm surge simulations, Ocean Eng., 243, 110233, https://doi.org/10.1016/j.apor.2021.103000, 2022.

Kalourazi, M. Y., Siadatmousavi, S. M., Yeganeh-Bakhtiary, A., and Jose, F.: WAVEWATCH-III source terms evaluation for optimizing hurricane wave modeling: A case study of Hurricane Ivan, Oceanologia, 63, 194–213, https://doi.org/10.1016/j.oceano.2020.12.001, 2021.

Lee, B. C., Fan, Y. M., Chuang, L. Z. H., and Kao, C. C.: Parametric sensitivity analysis of the WAVEWATCH III model, Terr. Atmos. Ocean. Sci., 20, 425–432, https://doi.org/10.3319/TAO.2008.04.25.01(Oc), 2009.

Li, Z., Li, S., Chen, J., Kong, Y., Fang, Y., Han, J., Zhu, P., and Hu, P.: Code and data for: A Generalized Framework for Multi-Parameter Optimization of Numerical Wind-Wave Model: Application to Typhoon Waves near Taiwan Island, Figshare [code and data set], https://doi.org/10.6084/m9.figshare.31236334, 2025.

Liu, Q., Babanin, A. V., Rogers, W. E., Zieger, S., Young, I. R., Bidlot, J. R., and Wang, J.: Global wave hindcasts using the observation-based source terms: Description and validation, J. Adv. Model. Earth Syst., 13, e2021MS002493, https://doi.org/10.1029/2021MS002493, 2021.

McKay, M. D., Beckman, R. J., and Conover, W. J.: A comparison of three methods for selecting values of input variables in the analysis of output from a computer code, Technometrics, 21, 239–245, https://doi.org/10.1080/00401706.1979.10489755, 1979.

Mentaschi, L., Besio, G., Cassola, F., and Mazzino, A.: Performance evaluation of Wavewatch III in the Mediterranean Sea, Ocean Model., 90, 82–94, https://doi.org/10.1016/j.ocemod.2015.04.003, 2015.

Pals, D., Schneider, T., and Stuart, A. M.: Targeted calibration to adjust stability biases in non-differentiable complex system models [preprint], 2024.

Raj, A., Kumar, B. P., Remya, P. G., Balakrishnan Nair, T. M., and Rohith, B.: Assessment of the forecasting potential of WAVEWATCH III model under different Indian Ocean wave conditions, J. Earth Syst. Sci., 132, 32, https://doi.org/10.1007/s12040-023-02045-w, 2023.

https://doi.org/10.5194/egusphere-2026-895
Preprint. Discussion started: 23 April 2026

Rogers, W. E., Babanin, A. V., and Wang, D. W.: Observation-consistent input and whitecapping dissipation in a model for wind-generated surface waves: Description and simple calculations, J. Atmos. Ocean. Technol., 29, 1329–1346, https://doi.org/10.1175/JTECH-D-11-00092.1, 2012.

Roh, M., Ha, K. J., and Yoo, J.: Sensitivity analysis of forecasting performance for ST6 parameterization in high-resolution wave model based on WAVEWATCH III, J. Mar. Sci. Eng., 11, 1038, https://doi.org/10.3390/jmse11051038, 2023.

Seemanth, M., Bhowmick, S. A., Kumar, R., and Sharma, R.: Sensitivity analysis of dissipation parameterizations in a third-generation spectral wave model, WAVEWATCH III for Indian Ocean, Ocean Eng., 124, 252–273, https://doi.org/10.1016/j.oceaneng.2016.07.023, 2016.

Song, Z. Y., Liu, H. L., Wang, F., Li, Y. Z., and Qiao, F. L.: Development and prospect of high-resolution ocean numerical models driven by big data, Adv. Mar. Sci., 37, 161–170, https://doi.org/10.3969/j.issn.1671-6647.2019.02.001, 2019 (in Chinese).

Soran, M. B., Amarouche, K., and Akpınar, A.: Spatial calibration of WAVEWATCH III model against satellite observations using different input and dissipation parameterizations in the Black Sea, Ocean Eng., 257, 111627, https://doi.org/10.1016/j.oceaneng.2022.111627, 2022.

Sun, R., Subramanian, A. C., Cornuelle, B. D., Mazloff, M. R., Miller, A. J., Ralph, F. M., Seo, H., and Hoteit, I.: Waves in SKRIPS: WAVEWATCH III coupling implementation and a case study of Tropical Cyclone Mekunu, Geosci. Model Dev., 16, 3435–3458, https://doi.org/10.5194/gmd-16-3435-2023, 2023.

WAMDIG (WAM Development and Implementation Group): The WAM model – A third generation ocean wave prediction model, J. Phys. Oceanogr., 18, 1775–1810, https://doi.org/10.1175/1520-0485(1988)018<1775:TWMTGO>2.0.CO;2, 1988.

WW3DG (The WAVEWATCH III Development Group): User manual and system documentation of WAVEWATCH III version 6.07, Tech. Note 329, NOAA/NWS/NCEP/MMAB, College Park, MD, USA, 326 pp. + Appendices, 2019.